Correcting the polarization effect in very low frequency dielectric spectroscopy

2009 J. Phys. D: Appl. Phys. 42 175505

(http://iopscience.iop.org/0022-3727/42/17/175505)

IOP PUBLISHING JOURNAL OF PHYSICS D: APPLIED PHYSICS

J. Phys. D: Appl. Phys. **42** (2009) 175505 (10pp) doi:10.1088/0022-3727/42/17/175505

Correcting the polarization effect in very low frequency dielectric spectroscopy

Camelia Prodan and Corina Bot

Physics Department, New Jersey Institute of Technology, Newark, NJ 07102, USA

Received 21 April 2009, in final form 21 July 2009
Published 17 August 2009
Online at stacks.iop.org/JPhysD/42/175505

Abstract

Polarization impedance appears at the interface between electrodes and ionic solutions and is a major source of errors in dielectric spectroscopy measurements. This work presents a simple, robust and automated methodology for measuring and analysing the polarization impedance of non-dispersive electrolytes, with a focus on the very low frequency domain from 1 Hz and up. The accuracy of the method is demonstrated by comparing the corrected dielectric permittivity and conductivity of various electrolytes either with their nominal values or with measurements taken with other high precision measuring devices. The dependence of the polarization impedance on several parameters, such as ionic concentration, applied voltage and separation distance between the electrodes, is also presented. For colloidal suspensions, it is argued that a modified protocol of the substitution method is needed due to several shortcomings occurring only in the very low frequency domain. Such a protocol is presented and tested on suspensions of live *E. coli* cells. As opposed to most of the existing methodologies for polarization removal, the proposed protocol makes no assumptions on the behaviour of the polarization impedance. This could potentially lead to the quantitative resolution of the α-dispersion of live cells in suspension.

(Some figures in this article are in colour only in the electronic version)

1. Introduction

Dielectric spectroscopy (DS) is a technique that measures the frequency dependent complex dielectric permittivity (DS curves) in order to extract useful information about the samples, to compare different samples and/or to study the changes occurring in the samples due to various factors. Because DS is noninvasive, it is widely used in many areas, including biophysics, pharmacology and geophysics [1–8]. The low frequency DS measurements are particularly interesting because most colloidal suspensions exhibit an α-relaxation in this frequency domain. The shape of the DS curves near the α-relaxation depends on the material composition and on the shape and size of the colloidal particles [9]. For live cell suspensions, the DS curves are also strongly dependent on the membrane and several other important cell parameters [10–12].

Unfortunately, the quantitative interpretation of the DS measurements is limited by the inherent electrode polarization effect. This manifests itself as the apparition of a polarization impedance at the interface between the electrode and the sample, due to the polarization of the ionic double layer forming at the interface. The effect is present at all frequencies, but it is stronger at low frequencies. To obtain the intrinsic DS curves of samples, the polarization effect has to be accounted for and removed from the data. This problem is of considerable interest to scientists from many areas of research, as indicated by the large amount of research published on this subject [13–19]. If this can be accomplished with a high degree of accuracy, the experimental DS data can be quantitatively analysed using various theoretical models [10–12, 20, 21] and one can extract absolute values, as opposed to relative values, for several parameters of great interest to scientists working with colloidal suspensions and live biological cells. This study is part of an effort towards resolving the α-region of DS curves for live cell suspensions, where most of the available experimental methods encounter difficulties (see the strong critiques of [22]).

This paper builds on the substitution technique, which was available for some time [17, 18, 23–25]. Our goal is threefold: (a) measure, (b) analyse and (c) remove the electrode polarization error at low frequencies, starting from 1 Hz and above. In the first part, we investigate samples with known dielectric behaviour such as saline solutions and buffers.

Here, we concentrate on the practical implementation side, with a focus on accuracy and making the method automated. Using the data on these systems, we map the dependence of the polarization impedance on different parameters such as frequency, applied voltage, electrode separation distance and ionic concentrations. Analysis of the data reveals that the polarization impedance is mainly reactive and that it has inverse power law behaviour with frequency. For one set of solutions, the extracted power law exponent is found to be in very good agreement with previous measurements. However, we find that the power law exponent is weakly dependent on the ionic concentration of the solution and that the polarization impedance can be quite different when comparing two sets of solutions with not so different ionic concentrations. The coefficient in front of the inverse power law is also found to depend on the ionic concentration, more precisely, to be inversely proportional to the conductivity of the solution. We find similar behaviour for HEPES, a widely used buffer in life sciences.

We also propose a modified protocol for the substitution method that allows unbiased measurement, analysis and removal of the electrode polarization for dilute colloidal suspensions. The polarization impedance is determined by the fluid in direct contact with the electrodes. Thus we argue that, at least for dilute colloidal suspensions, the polarization impedance is in fact generated by the medium surrounding the cells in suspension and therefore the polarization impedance can be extracted directly from the medium rather than from a reference electrolyte. Thus, the protocol bypasses the assumption that electrolytes of the same conductivity generate the same polarization impedance, leading to a completely unbiased method for polarization removal. This modified protocol also bypasses a practical problem related to the substitution method at very low frequencies, a problem that is described at the end of this section.

We discuss two practical methodologies for separating the medium and we report an application of the protocol to *E. coli* cells in aqueous suspensions. Corrected DS curves are presented for two cell concentrations. The measurements have been repeated for five different samples and the resulting error bars demonstrate the robustness and repeatability of the measurements. The DS curves display features that are in agreement with various theoretical models.

Let us end this section by briefly going through the existing methodologies for polarization removal and their successful applications to different systems. A detailed presentation of the existing electrode polarization removal methods can be found in the reviews of [24, 26, 27]. Several methodologies are based on the observation that, in the very low frequency range, the polarization impedance Z_p behaves as a frequency dependent RC circuit, with the resistor R_p and capacitor C_p in series and having the frequency dependent values: $C_p = A\omega^{-m}$, $R_p = B\omega^{-n}$ [28]. The parameters A, B, m and n depend on the electrode and electrolyte properties, as well as on their interaction. Since the polarization impedance is physically localized at the interface between the electrodes and the sample, Z_p can be set in series with the sample's impedance Z_s, to give the total measured impedance Z. In this context then, to remove the polarization errors, one has to develop methodologies for determining the parameters A, B, m and n that characterize the polarization impedance. A fitting methodology was designed and tested in [15]. This technique was successfully applied to obtain the DS curves for rat liver cells in the frequency range from 10^3 to 10^8 Hz. The authors of this study stated that it remains unclear whether the trends in the dispersion curves below 10^3 Hz are due to the α-effect or to an artefact related to insufficient polarization removal. The method just presented is sometimes mentioned under the name of frequency-derivative method.

A more elaborate procedure was proposed in [13], in which Z_p is parametrized as described above and in the same time, Z_s is parametrized using phenomenological frequency dependence functions. The result is a phenomenological fitting function for the total impedance, which is then used to fit the experimental dispersion curves on the entire range of frequencies, using a large number of fitting parameters. This methodology was successfully applied to describe the dielectric properties of erythrocytes in the frequency range from 1 kHz to 1 GHz. This methodology may be sensitive to the phenomenological function used to parametrize Z_s, and the results could be biased by a particular choice. For example, the methodology had difficulty in resolving the α-dispersion of any live cell suspension.

Distance variation technique is another method for polarization removal. We have used this method successfully in the past to remove the polarization error in low conductivity fluids such as pure water, toluene, glycol and for cells suspended in low conductivity buffers [29]. This methodology is based on the observation that Z_p is practically independent of the separation distance d between the capacitor's plates. Thus, by measuring the $Z = Z_s + Z_p$ for two values of d, one can eliminate Z_p by subtracting the results of the two measurements.

The substitution technique measures the polarization impedance using a reference electrolyte whose conductivity is adjusted to match the conductivity of the biological sample [17, 23]. Other works [25] proposed to use the supernatant as the reference electrolyte, which is the path we pursue in this work. This methodology was successfully implemented in the high frequency β-dispersion domain [17, 18], but at low frequencies, between 1 Hz and 1 kHz, it presents a problem since the true conductivity of the biological sample is not known until the polarization errors are removed. The polarization errors are extremely high and using the uncorrected data to determine the conductivity of the biological sample, so that one can adjust the properties of the reference electrolyte, will simply not work in practice because the conductivity obtained this way takes values that are clearly un-physical.

At the end, we should mention that the polarization errors can be reduced by using special electrodes, such as the fractal electrodes (platinum black is one example), or using gratings instead of flat electrodes. Most of these options have been tested in [22], one of the conclusions being that none of these techniques will totally eliminate the polarization error.

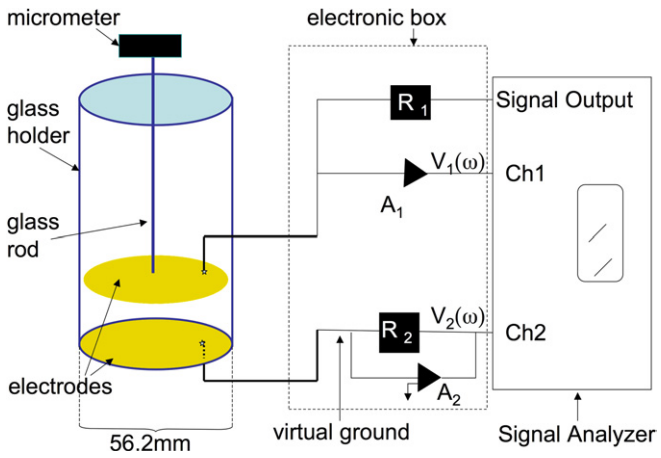

Figure 1. The experimental set-up used in this paper. The suspension is placed in a glass cylinder. Two gold plated, flat electrodes are immersed into the suspension. The distance between the electrodes is controlled by a micrometer. The signal analyzer applies a voltage on the upper electrode while the bottom one is kept at virtual ground through the negative input of an amplifier. The transfer function, i.e. the ratio between the voltages at channels 1 and 2, is recorded for each frequency and used to compute the complex dielectric function of the sample as explained in the text. (Colour online.)

2. Materials and method

2.1. Experimental set-up

We use the same experimental set-up as in [29], which is illustrated in figure 1. The sample to be measured is placed between two parallel gold plated electrodes (yellow) that are enclosed in a long cylindrical glass tube (dark blue). The results reported here were obtained with electrodes of 28.1 mm radius. In order to minimize the chemical reactions between the electrodes and the solution, gold, an inert metal, was plated on the electrodes. It was found that 100 nm was enough to withstand the corrosion from the salty buffers and other media used for live cells measurements. The distance between the capacitors plates is controlled with a micrometer. To reduce the errors due to the stray capacitance at the edges of the electrodes, the bottom electrode was made as large as the glass container and the upper electrode just 1 mm smaller, to allow the flow of the fluids when modifying the electrodes separation. Because of this choice, the stray electric field lines go mostly through the glass container (dielectric permittivity of 4) or air (dielectric permittivity of 1) and, since these are materials of reduced dielectric constant (compared with 78 of water), this reduces the contribution of stray capacitance to the measurements. The electrode guard technique for reducing the stray effects was also tested but no improvement was seen in the measurements. The distance between the electrode plates was varied from 1 to 10 mm.

The experimental set-up works as follows. The signal analyzer (we use both the SR 795 and the Solartron 1260), provides a sinusoidal voltage at its signal output. It also digitizes the voltage at channels 1 and 2 and takes the ratio of these two as a function of frequency. The real and imaginary parts of this ratio are stored on a computer. The bottom electrode plate was held at relative ground potential through the negative input of the amplifier A_2. The output voltage from the signal analyzer is applied to the upper electrode, through resistor R_1. As a result, the current I that flows through the sample produces a voltage V_1, equal to the product of I and impedance Z of the measuring cell. The voltage V_2 is equal to the product of I and resistance R_2. Thus the transfer function, T, is directly related to the measuring cell impedance by $T = R_2/Z$. R_2 was fixed at 100 Ω in these experiments. If the impedance Z were not contaminated by the polarization effects and other possible factors, then the complex dielectric function $\epsilon^* = \epsilon + \sigma/j\omega$ of the sample could be calculated from

$$Z = \frac{d/S}{\mathrm{j}\omega\epsilon^*} \qquad \text{or} \qquad \epsilon^* = \frac{d/S}{\mathrm{j}\omega R_2} Z, \tag{1}$$

where d represents the distance between the electrodes, S the surface area of one electrode, ϵ and σ are the dielectric permittivity and conductivity of the sample and $\omega = 2\pi f$, where f is the frequency of the applied signal.

The set-up used in this paper was previously shown to correctly measure samples with a wide range of relative dielectric permittivities, from 2 (toluene) all the way to 78 (water) [29]. Without correcting the polarization error, the set-up gives the correct value of ϵ^* for frequencies down to 10 Hz for non-polar liquids and down to 1 kHz for water.

2.2. E. coli *preparation*

In experiments with live cells, *E. coli* K12 wild type (www.atcc.com) were incubated in 3 ml of tryptone soy broth (growth media) at 175 rpm and 37 °C to the saturation phase for 16 h. They were then re-suspended in 60 ml of media and incubated for 5 h in the same conditions until they reached the mid-logarithmic phase. To determine the cell growth and concentration, a spectrophotometer was used to measure the optical density of the cell suspension before the measurements. For DS, a fresh suspension of cells was centrifuged at 2522 × g for 10 min before each measurement and the pellet re-suspended in ultrapure (Millipore) water with 5 mM glucose that is routinely used to balance the osmotic pressure.

To check cell viability in media and water, two methods, plate counting and membrane potential dyes, were employed. For plate counting, two test tubes with 10 ml of cells in media and cells in ultrapure water with 5 mM glucose were tested for a extended period of time. Each day, cells were cultivated on agar plates by serial dilutions and incubated for 18 h at 37 °C and the number of colonies counted from the smallest dilution area. The membrane potential dye, Di-SC3-5 carbocyanine iodide (www.anaspec.com), was used to stain the cell membrane and test for viability. The labelled cells were imaged using an inverted microscope, Axiovert by Zeiss, in the fluorescence mode. Dye was added in a concentration of 0.4 μM to cells in media and cells in water and imaging was performed after 15 min, to allow the dye to settle in the membrane. All measurements were done at 25 °C.

3. Measuring the polarization impedance

The polarization effect is due to the polarization of the ionic charges accumulated at the interface between the fluid and the metallic electrodes [17, 27, 30]. The polarization of the ionic double layer depends on the chemical and physical properties of the electrode as well as of the fluid that comes in contact with the electrodes. Because the effect takes place at the interface between the sample and the electrode, mostly within a few nanometres from the electrode, the polarization impedance Z_p appears in series with the intrinsic impedance of the sample Z_s. In other words, the measured impedance is the sum of the two: $Z = Z_s + Z_p$. Thus, if one develops a method to measure Z_p, the intrinsic impedance of the sample can be obtained by subtracting Z_p from the measured Z.

We will use Millipore water to exemplify a practical method to measure Z_p with extremely high accuracy. The dielectric function of pure water is known to be constant $\epsilon_r = 78$ (relative to the vacuum) for a frequency range spanning from 0 Hz to several GHz. However, if we use the raw DS data and compute the dielectric function using equation (1), we obtain the graph shown in figure 2(*k*) (red line, dot symbol). Looking at this graph, we see that from approximately 1 kHz and up, ϵ_r agrees extremely well with the nominal value of 78, while from 1 kHz down, ϵ_r deviates quite strongly from this value. The anomalous behaviour of ϵ_r at these low frequencies is the typical manifestation of the electrode polarization effects. This observation shows that above 1 kHz the effect is practically gone. If we plot the real and imaginary parts of the impedance Z (the red lines in figures 2(*a*) and (*f*)), and the intrinsic impedance of the Millipore water (the blue lines in figures 2(*a*) and (*f*)), computed as $d/\mathrm{j}\omega\epsilon^* S$, with ϵ^* being the nominal complex dielectric function of Millipore water, we see that the two graphs match quite well above 1 kHz. In fact, if we fit the experimental values of Z above 1 kHz with a frequency dependent function

$$Z_{\mathrm{fit}} = \frac{d/S}{\mathrm{j}\omega\epsilon + \sigma}, \tag{2}$$

with ϵ and σ as fitting parameters, we obtain $\epsilon = 78$ and $\sigma = 0.000\,070\ \mathrm{S\,m^{-1}}$, in perfect agreement with the nominal values of the Millipore water. Now, since it is known that the dielectric function and conductivity of ionic solutions are constant all the way to zero frequency, we can extrapolate Z_{fit} to lower frequencies. The difference between the measured Z and Z_{fit} is precisely the polarization impedance Z_p. Thus, we can measure in this way the polarization impedance and a plot of Z_p is shown in the inset of figure 2(*f*) (the green line).

Based on all the above, the following methodology emerges:

(i) Fit the experimental data for Z with the function Z_{fit} given in equation (2), by giving a large weight to the high frequency data and a low, or almost zero weight to the low frequency data. How to choose the high–low frequency domains depends on the sample at hand, the guiding principle being that the fitted curves should display an accurate match with the raw data in the adopted high frequency region. Of course, this requires a few preliminary measurements.

(ii) From the fit, determine the true dielectric constant ϵ and conductivity σ of the ionic solution.

(iii) Extrapolate Z_{fit} all the way to 0 Hz and obtain the intrinsic impedance Z_s of the ionic solution at low frequencies.

(iv) Compute Z_p as the difference between Z and the extrapolated Z_s.

All data on Z_p reported in this paper were obtained by an automated implementation of the above four steps. Figure 2 shows an application of the above procedure to a series of weak saline solutions, which will be analysed later in the paper.

4. Characterization of Z_p

We will use the Millipore water to answer several important questions about the polarization impedance. The methodology outlined above was applied for three values of the distance between capacitor plates, $d = 1$, 3 and 5 mm. For each d, the experiments were repeated for five values of applied voltages per centimetre: 0.1, 0.3, 0.5, 0.7 and 0.9 V cm^{-1}. Steps (i)–(iv) listed above were applied to the resulting 30 measurements.

The results are presented in figure 3. In the first row of this figure, one can see $\mathrm{Re}[Z_{\mathrm{fit}}]$ almost overlapping with $\mathrm{Re}[Z]$, while in the second row one can see a large difference between $\mathrm{Im}[Z_{\mathrm{fit}}]$ and $\mathrm{Im}[Z]$. Thus, our first finding is that Z_p is mostly reactive. This confirms the assumption on Z_p made on [13] that the coefficient A can be set to zero. The insets in figure 3 show $\mathrm{Im}[Z_p]$ as a function of frequency in a log–log scale, for various values of d and applied electric fields. The $\mathrm{Im}[Z_p]$ was obtained from the main plots by taking the difference $\mathrm{Im}[Z_p] = \mathrm{Im}[Z] - \mathrm{Im}[Z_{\mathrm{fit}}]$. The log–log plots appear as straight lines for a wide range of frequencies, the fact that confirms the power law behaviour of $\mathrm{Im}[Z_p]$ with the frequency. The exponent of the power law can be easily and accurately obtained from the plots and will be discussed later in the paper. Analysing the insets, we observe a weak dependence of $\mathrm{Im}[Z_p]$ on the applied electric field. The shape of the curves changes slightly as the electric field is varied and the effect seems to be more pronounced for the smallest value of d. For larger d, the effect is almost nonexistent, which supports the assumption that the amplitude and the exponent of the power law are independent of the applied electric field. Also, we observe almost no dependence of Z_p on the distance between the electrodes.

5. Robustness of the methodology

5.1. Weak ionic solutions

In figure 2 we present an application of the methodology to electrolytes with low conductivity, more precisely, water with low concentrations of KCl. From left to right, the different columns refer to 0, 1, 5, 10 and 20 μM KCl. For low KCl concentration, the dielectric function of the solution remains constant at 78, while large increases in the conductivity can be observed. In all columns of figure 2, we can see an almost perfect match between the real parts of Z and Z_{fit}. The fit is also perfect for the imaginary parts of Z and Z_{fit}, if we look above 1 kHz. The fitting provided the following values: $\epsilon_r = 78 \pm 1$

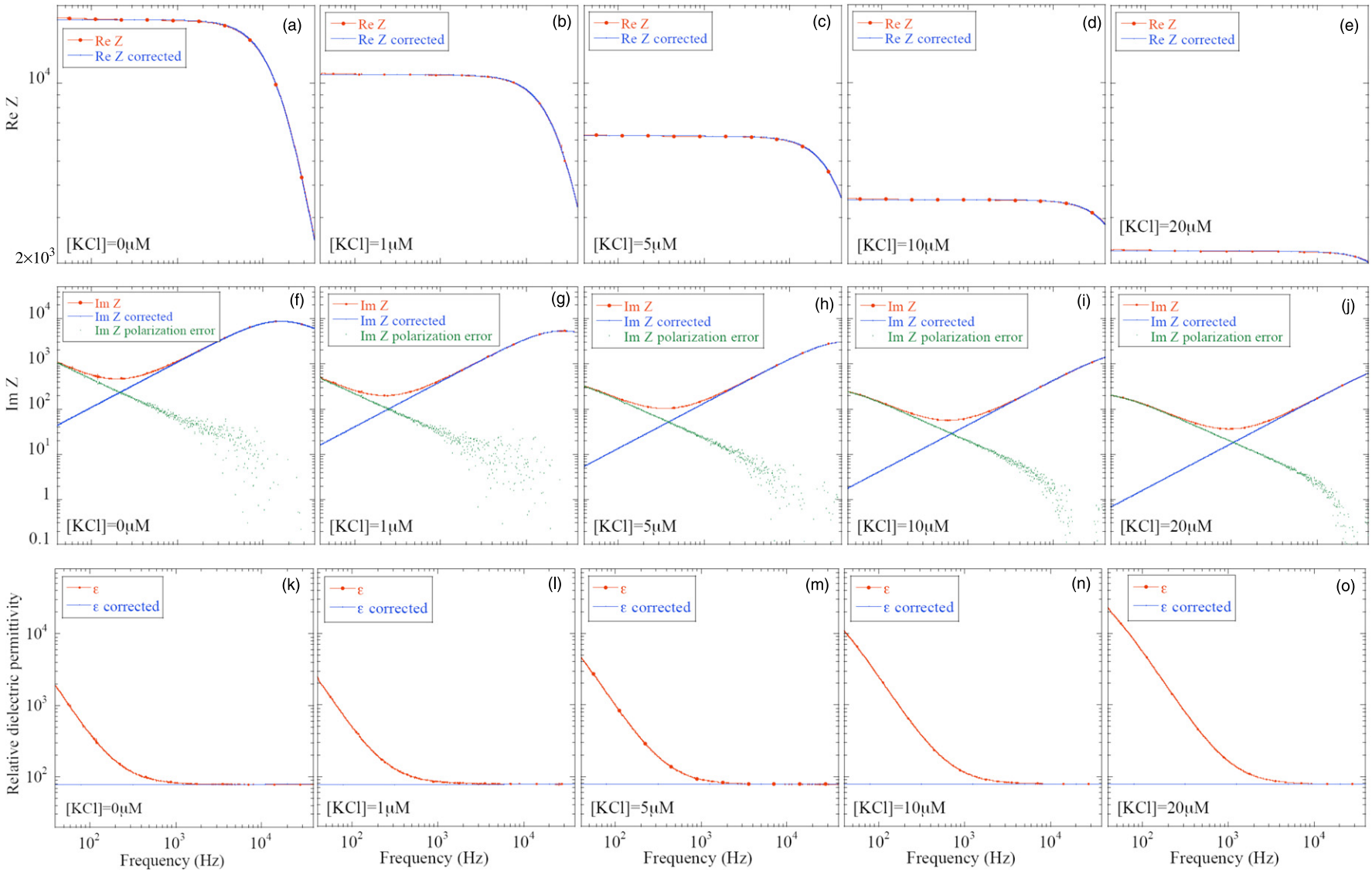

Figure 2. DS measurements for Millipore water with 0, 1, 5, 10 and 20 μM KCl. Panels (*a*)–(*e*) show the real part of the impedances; panels (*f*)–(*j*) show the imaginary part of the impedances; panels (*k*)–(*o*) show the corrected and uncorrected dielectric permittivities.

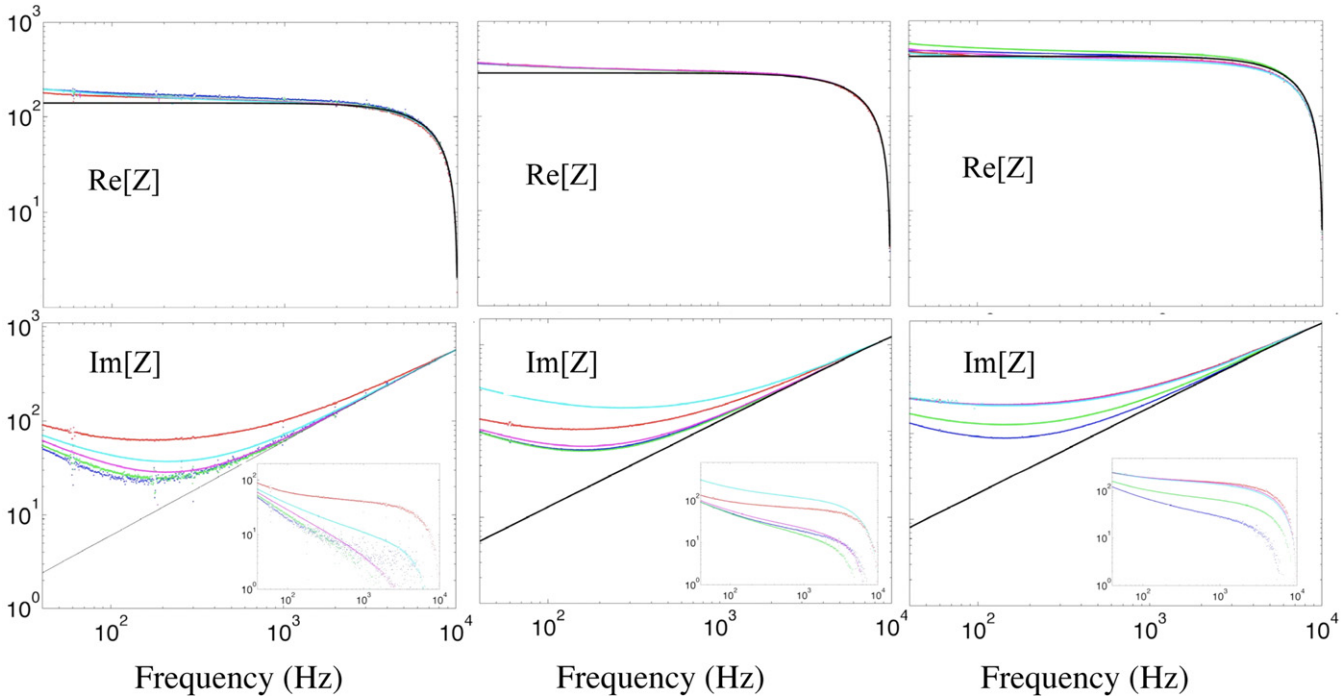

Figure 3. Real (1st row) and imaginary (2nd row) parts of the total impedance for $d = 1$ mm (1st column), $d = 3$ mm (2nd column) and $d = 5$ mm (3rd column), for applied electric fields of 0.1 (red), 0.3 (blue), 0.5 (green), 0.7 (magenta) and 0.9 (cyan) V cm^{-1}. Black line marks Z_{fit}. The insets show the corresponding Im[Z_{p}]. (Colour online.)

and $\sigma = 0.000\,11\,\text{S m}^{-1}$, $0.000\,20\,\text{S m}^{-1}$, $0.000\,34\,\text{S m}^{-1}$ and $0.000\,56\,\text{S m}^{-1}$ for the four cases, respectively. To these significant digits, the same values of σ have been measured using a precision conductivity probe, the Denver Instruments Model 220. This demonstrates that, by an automated implementation of steps (i)–(iv) described above, we were able to remove the polarization effects and obtain the intrinsic dielectric function and conductivity of all these solutions with extremely high accuracy.

5.2. *Stronger ionic solutions*

Low frequency DS has applications in many fields, but we are primarily interested in biological applications, such as measuring the dielectric functions of live cell suspensions. Many physiological buffers are known to have high conductivities. Thus, in order to apply our method to live cells in suspension, we must demonstrate that it works for strong ionic solutions.

As the conductivity of the electrolyte increases so does the frequency limit where the polarization effect highly contaminates the data. Since our method relies on the information contained in the high frequency domain where the polarization effects are small, the experimental data must contain a good part of this domain. Thus, for strong ionic solutions, we need to record the DS curves up to much higher frequencies. This is why, in the experiments with strong ionic solutions we replaced the initial signal analyzer SR 795 with the Solartron 1260, which allowed us to record data in the frequency window from 0 Hz to 1 MHz.

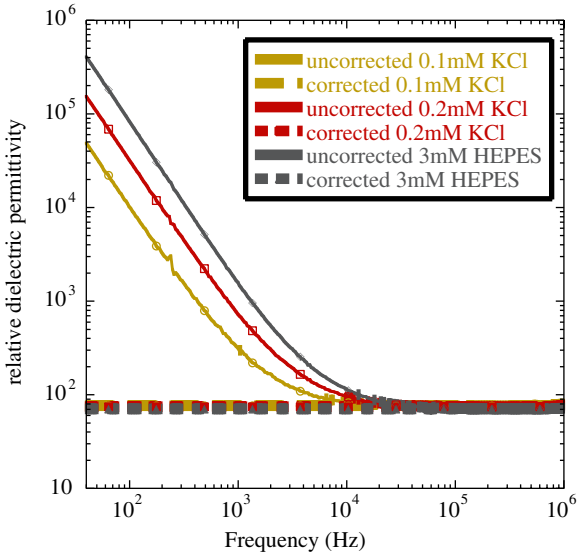

Figure 4. Dielectric permittivity versus frequency for water with 0.1 and 0.2 mM KCl and 3 mM HEPES. The dotted lines represent the intrinsic relative dielectric permittivity, obtained after correcting the polarization error.

We give an application of the methodology to water and KCl, at much higher concentrations than before, namely 0.1 and 0.2 mM KCl concentrations, and to HEPES of 3 mM concentrations. The dielectric functions before and after polarization removal are shown in figure 4. For the two KCl solutions, the methodology provides the following values: $\epsilon_{\text{r}} = 76 \pm 0.07$ and $\sigma = 0.001\,71\,\text{S m}^{-1}$ (0.1 mM),

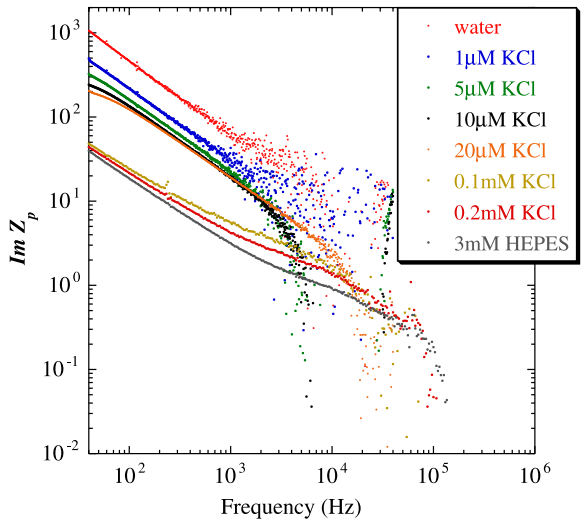

Figure 5. Im$[Z_p]$ for the samples reported in figures 2 and 4 as a function of frequency. The curves display a power law behaviour with an average exponent of 0.8 (0.6) for the manifold of curves corresponding to μM KCl (mM KCl) concentrations and of 0.5 for HEPES.

$\epsilon_r = 75.54 \pm 0.08$ and $\sigma = 0.003\,24\,\mathrm{S\,m^{-1}}$ (0.2 mM). For HEPES solutions, the methodology provides $\epsilon_r = 75.2$ and $\sigma = 0.007\,50\,\mathrm{S\,m^{-1}}$ (35 mM). Again, to these significant digits, the same values of σ have been measured using the conductivity probe. According to our measurements, the dielectric constant of the KCl solution decreases with the KCl concentration. This is an effect that has been discussed before in [31, 32]. The effect has been quantified in a series of very precise measurements in the GHz frequency range [33]. When extrapolating to low frequencies by using a single Cole–Cole equation, [33] finds a linear drop in ϵ_r with the KCl concentration of the solution, a behaviour that was correlated with the polarization of the hydration shells of the ions. Our data show a slightly stronger linear drop than the one seen in [33].

5.3. Behaviour of Z_p with the ionic concentration

Now we can say a few things about the behaviour of Z_p with the increase in KCl concentration. In figure 5 we put together the Im$[Z_p]$ reported in figures 2 and 4. Looking at figure 5, one can see two manifolds of curves, corresponding to the low and the high KCl concentrations. The manifold of low KCl concentrations is higher and more spread out when compared with the manifold for higher KCl concentrations. All curves show a consistent decrease in Im$[Z_p]$ with the increase in KCl concentration. Quantitative analysis of this decrease shows that Im$[Z_p]$ is *inversely proportional to the KCl concentration*, in line with theoretical studies that also found Im$[Z_p]$ to be inversely proportional to the conductivity of the electrolyte [13, 30]. This also explains why the manifold of curves for low KCl concentrations is more spread out.

Another finding is that the exponent α of the inverse power law behaviour Im$[Z] \propto \omega^{-\alpha}$ *decreases* with the increase in KCl concentrations. This decrease is visible even within each manifold. Quantitatively, we find an average of $\alpha = 0.8$ for low KCl and an average of $\alpha = 0.66$ for higher KCl concentrations. The last value is in line with a previous study [13], which found an exponent of $\alpha = 0.7$ for mM KCl concentrations. Figure 5 also presents Im$[Z_p]$ for a HEPES buffer for which we find an α of 0.75.

6. Polarization effects in colloidal suspensions

We should point out from the beginning that the dielectric functions of colloidal suspensions are not constant with frequency. In fact, the main goal of DS is to capture and study these variations with frequency. Thus, the methodology studied in the previous sections cannot be directly applied to these systems. One practical solution used in the past was to measure Z_p using an electrolyte that has similar conductivity as the colloidal suspension. Most often, this reference electrolyte was a simple saline solution with the KCl concentration adjusted accordingly. The assumption was that electrolytes with the same conductivity generate same polarization impedances, which we have seen may not always be the case at very low frequencies. An even more stringent problem, which renders this solution inapplicable at frequencies below 1 kHz, is the fact that we do not know how to get the conductivity of the colloidal suspension in the first place. Using the uncorrected DS curves leads to spurious values for conductivity.

Let us elaborate the last point and explain what is different for frequencies below 1 KHz. One of our earlier conclusions was that Z_p is mainly reactive and for that reason it does not affect the real part of the impedance of the sample. The data of figure 2 confirm that this is indeed the case. Moreover, one can see in this figure that Re$[Z]$ becomes practically constant below 1 KHz, and this is because $\mathrm{Re}[Z_s] = \sigma d/A(\omega^2\epsilon^2 + \sigma^2)$ rapidly converges to $\mathrm{Re}[Z_s] \to d/A\sigma$ in the low frequency domain. Thus, one can, in principle, extract σ from the raw data of the real part of Z, thought, in practice, we find that one needs both real and imaginary parts of Z_s to achieve the accuracies we previously described. Nevertheless, there is no major problem in obtaining a relatively good value of σ for non-dispersive electrolytes. Now let us turn our attention to the colloids. In figure 6, we show the raw data for Re$[Z]$ for *E. coli* cells in suspension. As one can see, the situation is different. The plateau seen for non-dispersive electrolytes is no longer there. The new behaviour is due to the fact that σ is dispersive for colloids, but more importantly, because ϵ takes extremely large values at lower frequencies, therefore the convergence $\mathrm{Re}[Z_s] \to d/A\sigma$ is not valid anymore. Consequently, one needs both Re$[Z]$ and the *corrected* Im$[Z]$ to determine σ and ϵ, which must be done simultaneously. It is clear that at frequencies below 1 kHz we need to modify the substitution method.

According to the modern theory of polarization impedance [30], the impedance is determined solely by the fluid that is in direct contact with the electrodes. The thickness of the electrical double layer responsible for the polarization error is contained within a few nanometres from the electrode. In our experiments, the applied electric field is kept small and for that

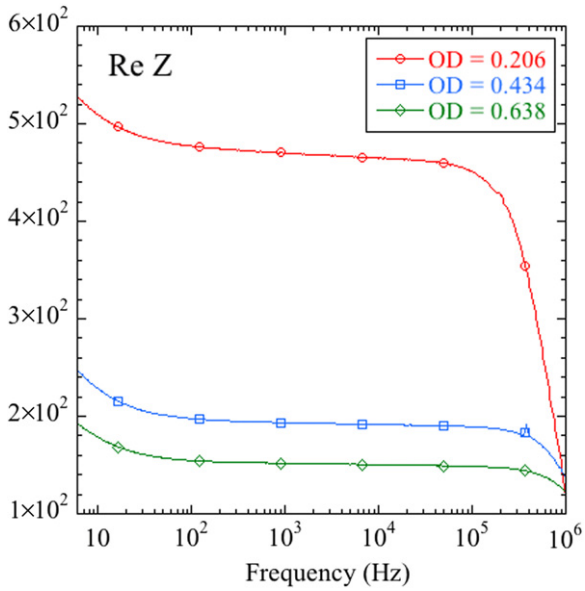

Figure 6. The real part of the measured impedance Z for three cell concentrations. Note the dispersive behaviour along the entire range of frequencies.

reason we do not observe any migration and accumulation of the cells towards the electrodes. Also, the cell concentrations are relatively small, therefore the average number of cells in the electrical double layer is practically zero. Thus, the fluid that is in direct contact with the electrodes is just the medium in which the cells are suspended. Therefore, if we separate the medium from the colloids, we can measure Z_p directly on the medium, which can then be removed from Z to obtain the intrinsic impedance of the sample. It is important to note that, when cells are suspended in a medium, they modify the dielectric properties of the medium by releasing ions through an ion-exchange process needed to stabilize their membrane potential. Thus, we must measure the medium after the cells have been suspended. Given all these, the following protocol emerges:

(I) Record the raw values of Z.
(II) Gently remove the colloids from the solution and save the supernatant. Extra care is needed when working with cells suspensions since cells can break during centrifugation leading to an increase in the conductivity. This step could be eliminated by using the set-up from figure 7.
(III) Apply steps (i)–(iv) to the supernatant and determine Z_p.
(IV) Remove Z_p from Z to obtain the intrinsic impedance of the sample.

Although the following observation is not pursued in this work, we want to point out that the protocol (I)–(IV) can be applied in one step, i.e. the medium and the colloidal suspension can be measured simultaneously. For mammalian cells that are large in size, for example, it is possible to divide the measuring cell into two compartments, using a membrane that is permeable to the medium but not to the live cells. The resulting measuring cell is illustrated in figure 7, and such a measuring cell will separate the medium with the same

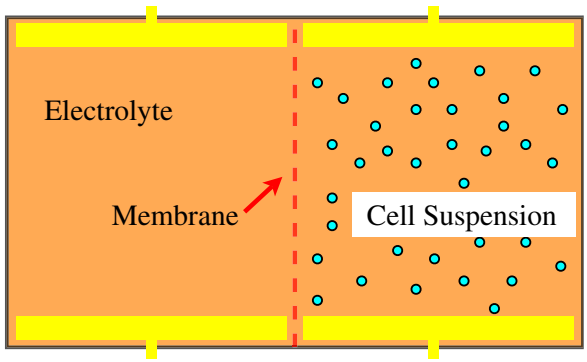

Figure 7. A measuring cell that will allow simultaneous DS measurements of the live cells suspension (using the right capacitor) and electrolyte (using the left capacitor).

ionic properties as that surrounding the cells, thus allowing simultaneous DS measurements for the cell suspension and for the medium. The measuring cell shown in figure 7 is easy to construct for geophysical applications where one is interested in the dielectric properties of granular soils, with granules typically of millimetre or slightly sub-millimetre sizes. We can argue that such a measuring cell will be superior to the measuring cells used in the distance variation technique because there are no moving parts and because we can obtain the value of Z_p, which is an interesting quantity in itself.

Since the mamalian cells are tedious and expensive to grow, we show here an application of the above protocol to live *E. coli* cell suspensions. *E. coli* cells are 2 to 5 μm in size so the measuring cell illustrated in figure 7 is not feasible. Instead, we chose to implement the protocol (I)–(V) in two steps. For this, we first take the DS measurements on the *E. coli* suspension and then separate the supernatant by gentle centrifugation and subject it to the DS measurements. The *E.coli* cells were harvested in their mid logarithmic phase then re-suspended for measurements in ultra pure water plus 5 mM glucose (for osmotic pressure balancing) at an OD $= 0.186$. The ultra pure water was our choice because it has a low conductivity and therefore we could avoid the technical problems related to high conductivity media, explained in the previous section. This is is an important detail, since the conductivity of the medium controls the position of the β-dispersion, which, as we shall see, is moved to the lower frequencies when compared with other experiments. The samples were prepared as explained in section 2. The same section also describes our tests on the cell suspension viability to make sure that the cellular suspensions were healthy. The measurements were taken with a distance between the electrode plates of 3 mm.

Various available models indicate that at high frequencies, above the β-dispersion, the conductivity of the cell suspension should become comparable to that of the medium surrounding the cells. The same rule applies to dielectric permittivity. Thus, by comparing the high frequency impedances of the suspension and of the supernatant, we can quantitatively assess how effective was the separation process. During the experiments, we observed that if the cells were not carefully spun, the ionic properties of the supernatant can be different from that of the cell suspension, and we can tell that because the high frequency

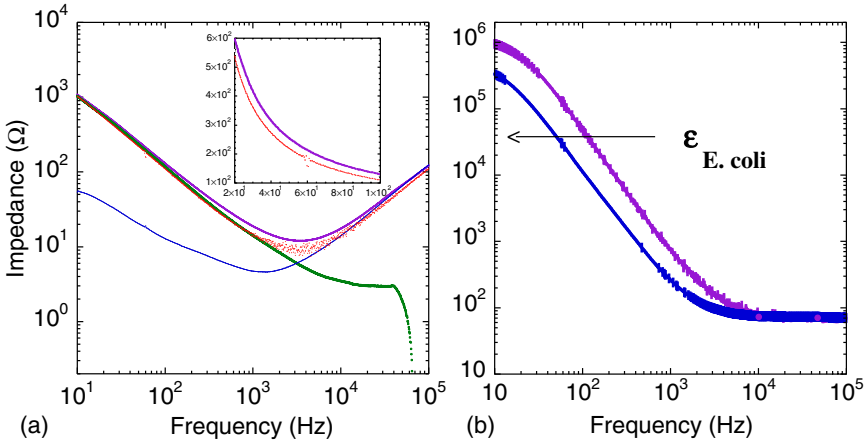

Figure 8. Dispersion curves for *E. coli* at OD = 0.186. Left: the imaginary part of the measured impedance Z of the cell suspension (mangenta), of the supernatant (red), of the polarization impedance Z_p (green) and of the corrected (intrinsic)impedance Z_p of the sample (blue). Right: the dielectric curves for the cell suspension before (mangenta) and after the correction for the electrode polarization impedance (blue) done using the technique presented in this paper. (Colour online.)

conductivity of the supernatant was much higher than that of the cell suspension, suggesting that ions were released in the medium during the centrifugation. When the centrifugation speed was reduced, the conductivity of the supernatant came closer and closer to that of the cell suspension. In the final protocol, cells were centrifuged at 2522 × g for 2 min and the supernatant was collected for the first time. The supernatant was centrifuged again for 2 min and collected for the second time and then centrifuged again for another 4 min.

As one can see in figure 8(a), there is a good overlap between the Z suspension and the Z supernatant at high frequencies, as one should expect. This is our experimental evidence that the supernatant has the same ionic properties as the medium surrounding the cells in suspension. Consequently, the polarization of the double layer near the electrodes should be similar for the two cases. We also provide error bars for our measurements, from which one can determine the fluctuations induced by the two-step implementation. We mention that the error bars are small enough to allow quantitative evaluations of the membrane potential during various induced physiological changes in the *E. coli* cells as we show in [34].

In figure 8(a), we present the raw values (magenta) of the imaginary part of the measured impedance Z and that of the impedance of the supernatant (red) obtained by extremely gentle centrifugation. The inset gives a detailed picture of the data in the frequency range from 20 to 100 Hz, plotted in a lin–lin scale. The plot shows a substantial difference between the two sets of data (of more than 5%), a difference that can be easily resolved by our electronic set-up. The green line in figure 8(a) represents the imaginary part of Z_p determined from the DS measurements on the supernatant as explained in the (I)–(IV) protocol. The blue line represents the imaginary part of the intrinsic impedance Z_s of the cell suspension.

Figure 8(b) shows the dielectric permittivity of the *E. coli* suspension as computed from Z (magenta) and computed from Z_p (blue). The blue line represents the intrinsic DS curve of the sample. Figure 9 shows the intrinsic DS curve of two *E. coli*

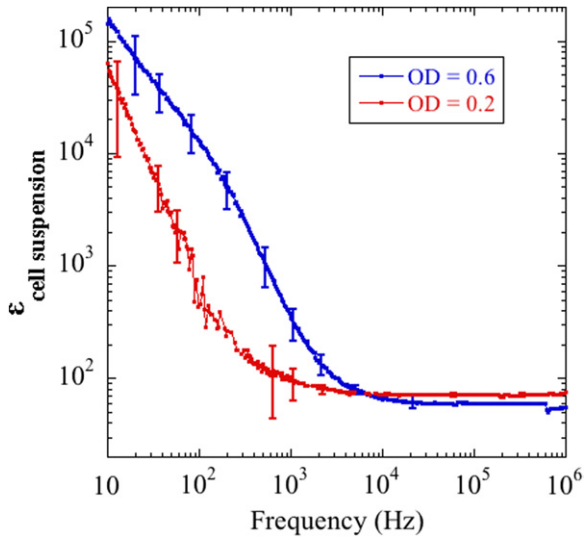

Figure 9. The dielectric curves for two cell suspensions of different volume concentrations. The error bars were obtained by repeating the DS measurements on five fresh samples. (Colour online.)

solutions of different volume concentrations, each obtained by averaging five independent measurements on five separate samples. The figure also shows the error bars resulting from the five measurements. As one can see, the error bars are small enough to allow the resolution of the two concentrations. A complete analysis, including comparisons with the existing theoretical models [10, 12] is given in [34]. In this reference we show that the experimental DS curves are in line with the theory and that we can obtain quantitative values for the membrane potential of the *E. coli* cells in suspension that are in line with other measurements.

Examining figures 8 and 9, we can distinguish a very high plateau in the DS curve, which we identify with the α-plateau [10, 12]. An intriguing feature of the DS curves is the absence of the β-plateau. To explain the absence of the β-plateau, we recall our previous observation that the cells were suspended

in pure water of extremely low conductivity. The dielectric dispersion curves of cell suspensions are very sensitive to the conductivity of the medium. In particular, the β-dispersion shifts to the lower frequencies as this conductivity is decreased [10, 12]. Since the cells were suspended in pure water, the β-dispersion should be substantially shifted to the left, when compared with the previous experiments. For example, the β dispersion of *E. coli* solutions was measured in [35] and found to be between 10^5–10^6 Hz. In these experiments, the cells were suspended in a growth medium with a conductivity of about 440 times larger than that of the water used in our experiments. Using a well established model of the β response [36], we found that when lowering the conductivity by 440 times, the β dispersion moves from 10^5–10^6 Hz in the region where we observe the α plateau. This calculation is extensively discussed in [34]). Thus, in our experiments, the β dispersion is covered by the α dispersion due to the low conductivity of the medium in which the cells were suspended.

7. Conclusions

In the first part of our work we presented a practical methodology to measure, analyse and remove the polarization impedance Z_p for non-dispersive electrolytes. The high accuracy of the method was demonstrated by comparing the corrected dielectric functions for various electrolytes with nominal values or with measurements taken with other highly accurate devices. Using this methodology, we mapped the dependence of Z_p on various parameters, such as ionic concentration, applied voltage and electrode distance. Our study experimentally confirmed several theoretical predictions, such as the fact that the polarization impedance is reactive and that it varies as an inverse power law with frequency for monovalent ionic solutions. Our study also showed that the amplitude and the exponent of the power law are very weakly dependent on the applied voltage. We found that the exponent of the power law and the amplitude decreases with the increase in ionic concentration in quantitative agreement with previous works. By comparing two different types of solutions that have similar conductivities, KCl and HEPES, we saw that the polarization impedance can have different behaviours at very low frequencies. Thus, we pointed out that one must be careful with the assumptions made on the polarization impedance when trying to remove it.

For colloidal suspensions, we pointed out several shortcomings of the substitution method, which become unreliable in the very low domain of frequencies and we argued for the need for a modified protocol. We propose the protocol (I)–(IV), which we tested on suspensions of live *E. coli* cells. We argued that the protocol can be implemented in one step by using the measuring cell shown in figure 7 and such implementation is currently under investigation. In this work, we demonstrated a two-step implementation, in which the cells are removed by gentle centrifugation and the resulting supernatant is used to measure Z_p. We have presented evidence that, by gentle centrifugation, the resulting supernatant retains the same ionic properties as that of the medium surrounding the cells in suspension. We also presented evidence that the two-step implementation is robust and repeatable, leading to small error bars even when the measurements are repeated on completely new samples.

Obtaining uncontaminated DS data in the α-region opens the possibility of many interesting applications, the most notable being measuring the membrane potential as predicted in [10, 12].

Acknowledgment

This work was supported by a grant from the NJIT-ADVANCE that is funded by the National Science Foundation (Grant No 0547427).

References

[1] Leung G *et al* 2005 *J. Ass. Lab. Autom.* **10** 258–69
[2] Nawarathna D *et al* 2005 *Appl. Phys. Lett.* **86** 023902
[3] Nawarathna D, Miller J H and Claycomb J 2005 *Phys. Rev. Lett.* **95** 158103
[4] Facer G R, Notterman D A and Sohn L L 2001 *Appl. Phys. Lett.* **78** 996
[5] Keese C R *et al* 2004 *Proc. Natl Acad. Sci.* **101** 1554
[6] Sohn L L *et al* 2000 *Proc. Natl Acad. Sci.* **97** 10687
[7] Slater L, Ntarlagiannis D and Wishart D 2007 *Geophysics* **71** A1
[8] Slater L *et al* 2007 *Geophys. Res. Lett.* **34** L21404
[9] Carrique F, Ruiz-Reina E, Arroyo F J, Jimenez M L and Delgado A V 2008 *Langmuir* **24** 11544–55
[10] Prodan C and Prodan E 1999 *J. Phys. D: Appl. Phys.* **32** 335
[11] Grozze C and Shilov V 2007 *J. Colloids Interface Sci.* **309** 283
[12] Prodan E, Prodan C and Miller J H 2008 *Biophys. J.* **95** 1
[13] Bordi F, Cametti C and Gili T 2001 *Bioelectrochemistry* **54** 53
[14] Davey C L and Kell D 1998 *Bioelectrochem. Bioenerg.* **46** 91
[15] Raicu V, Saibara T and Irimajiri A 1998 *Bioelectrochem. Bioenerg.* **48** 325
[16] Schwan H P and Ferris C D 1968 *Rev. Sci. Instrum.* **39** 481
[17] Davey C L, Markx G H and Kell D B 1990 *Eur. Biophys. J.* **18** 255–65
[18] Davey C L, Davey H M and Kell D B 1992 *Bioelectrochem. Bioenerg.* **28** 319–40
[19] Sanabria H and Miller J H 2006 *Phys. Rev.* E **74** 051505
[20] Gimsa J and Wachner D 1998 *Biophys. J.* **75** 1107
[21] Carrique F *et al* 2007 *J. Chem. Phys.* **126** 104903
[22] Umino M, Oda N and Yasuhara Y 2002 *Med. Biol. Eng. Compu.* **40** 533
[23] Schwan H P 1963 *Physical Techniques in Biological Research* vol VIB (New York: Academic) pp 323–407
[24] Feldman Y, Polygalov E, Ermolina I, Polevaya Y and Tsentsiper B 2001 *Meas. Sci. Technol.* **12** 1355–64
[25] Lisin R, Ginzburg B Z, Schlesinger M and Y Y F 1996 *Biochim. Biophys. Acta* **1280** 34
[26] Stoneman M R *et al* 2007 *Phys. Med. Biol.* **52** 6589
[27] Kaatze U and Feldman Y 2006 *Meas. Sci. Technol.* **17** R17
[28] Schwan H P 1968 *Ann. New York Acad. Sci.* **148** 191
[29] Prodan C *et al* 2004 *J. Appl. Phys.* **95** 3754
[30] Schedier W 1975 *J. Phys. Chem.* **79** 127–36
[31] Fawcett W R 2004 *Liquids, Solutions and Interfaces* (New York: Oxford University Press)
[32] Hasted J B 1973 *Aqueous Dielectrics* (London: Chapman and Hall)
[33] Chen T, Hefter G and Buchner R 2003 *J. Phys. Chem.* A **107** 4025–31
[34] Bot C and Prodan C 2009 *Eur. Biophys. J.* at press
[35] Bai W, Zhao K and Asami K 2006 *Biophys. Chem.* **122** 136–42
[36] Asami K 1980 *Japan J. Appl. Phys.* **19** 359